Molecular simulations of liquid aliphatic carboxylic acids (C1-C6) using the 3D-RISM-KH molecular solvation theory

Roy, Dipankar; Kovalenko, Andriy

Publisher's version / Version de l'éditeur:
https://doi.org/10.1016/j.molliq.2022.120825
Journal of Molecular Liquids, 368, PB, 2022-11-19

Molecular Simulations of Liquid Aliphatic Carboxylic Acids (C1-C6) using the 3D-RISM-KH Molecular Solvation Theory

Dipankar Roy,[1] Andriy Kovalenko[2,3,*]

[1] Department of Mechanical Engineering, University of Alberta, 10-203 Donadeo Innovation Centre for Engineering, 9211-116 Street NW, Edmonton, Alberta T6G 1H9, Canada

[2] Department of Biological Sciences, University of Alberta, Edmonton, Alberta T6G 2E9, Canada

[3] Nanotechnology Research Centre, National Research Council of Canada, 11421 Saskatchewan Drive, Edmonton, Alberta T6G 2M9, Canada

Corresponding Author:

* E-mail: andriy.kovalenko@ualberta.ca

ORCID:

DR: 0000-0002-4703-0130

AK: 0000-0001-5033-4314

Abstract

The liquid structures of short straight chain aliphatic carboxylic acids (C1-C6) and halogenated acetic acids (trifluoro and trichloro) are analyzed with molecular dynamics simulations, three-dimensional reference interaction site model, and density functional theory calculations. The neat acids are found to exist in multimeric ordered form consisting of both open chain and cyclic oligomers. Introduction of water breaks the hydrogen bonding networks between adjacent acetic acid molecules by inserting water as a bridging molecule. The electronic structure calculations confirm the formation of chain and ring type structures in the liquid state.

Keywords: Aliphatic Carboxylic Acids; Aqueous Mixture; Molecular Solvation Theory; Three-Dimensional Reference Interaction Site Model; Molecular Dynamics; Density Functional Theory

Highlights

- Liquid straight chain aliphatic carboxylic acids were studied with various computational methods
- Ordered multimeric structures were found to exist in the bulk liquids for liquid acids
- All-atom MD and united atom RISM calculations provided comparable distributions of solvent sites
- Hydrated forms of the acetic acid and perhalo acetic acids were explored
- Density functional theory calculations provide structural insights of the neat and hydrated acid clusters

1. Introduction

Carboxylic acids play an important part in chemistry and biology with wide occurrences, e.g. amino acids, fatty acids, inorganic and organic esters, etc. The most common type of organic acids are carboxylic acids, and they generally have higher boiling point than water owing to intermolecular hydrogen bonding. The saturated homologues of carboxylic acids are found in nature. The unsaturated carboxylic acids have major industrial application as polymer building blocks. The smallest of the carboxylic acid, formic acid (FA), can be found in insect stings and has interesting stellar chemistry [1,2]. The higher homologues, viz. acetic acid (AA), propanoic acid (PA), butanoic acid (BA), Pentanoic acid (VA), and hexanoic acid (HA), have distinctive smell and can be found in milk products, plant extracts, and as fermentation byproducts. The aqueous solution of acetic acid is known as vinegar. The structure of liquid carboxylic acid has received attention due to their presence in biological membranes in ester form as well as model systems to study intermolecular hydrogen bonds in model systems [3-6]. In this manuscript, we have chosen six early homologues of the aliphatic saturated carboxylic acids (C1-C6), trifluoroacetic acid (TFA), and trichloroacetic acid (TCA) to model liquid state of carboxylic acid (Figure 1). Though several molecular simulations studies were reported for formic and acetic acids under various conditions [7-9], systematic simulations studies of the liquid states of the short chain carboxylic acids are conspicuously absent in chemical literature.

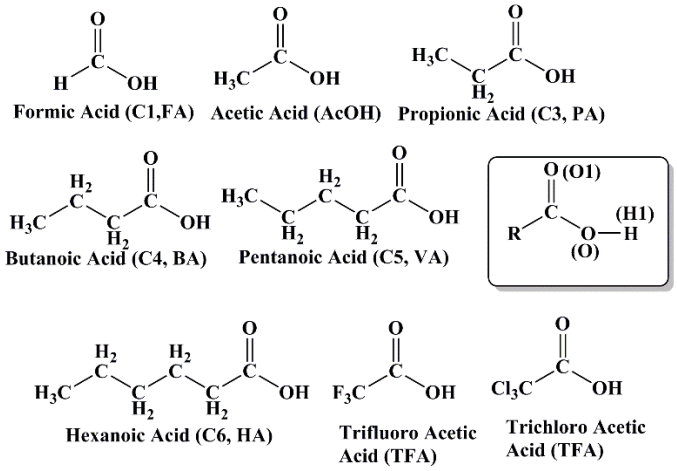

Figure 1. Carboxylic acids used in liquid state simulations in this work, and the atom numbering used.

The simulation of liquid states is accomplished by different well-established computational techniques, e.g. molecular dynamics simulations, Monte-Carlo simulations, first principle methods, etc. The reference interaction site model (RISM) of liquids is based on first principle statistical mechanics of molecular solvation theory. The theoretical

framework of RISM was established in the works of Chandler and coworkers. For detailed theoretical derivations behind the RISM formalism, see references [10-16]. Briefly, the 3D-RISM theory provides probability density of all possible interaction sites (γ) of solvent molecules around a solute of arbitrary shape at position r, as a product of the average number density ρ_γ in the bulk solution and the normalized density distribution $g_\gamma(r)$. The total correlation function (h_γ) is obtained from the direct correlation function c_γ and the site-site bulk susceptibility function (χ) for α solvent sites around a solute by the 3D-RISM integral equation:

$$h_\gamma(\boldsymbol{r}) = \sum_\alpha \int d\boldsymbol{r}' c_\alpha(\boldsymbol{r} - \boldsymbol{r}')\chi_{\alpha\gamma}(r') \ .$$

A closure relation is required to imposes a set of consistency conditions of the path-independent chemical potential μ and to obtain total and direct correlation functions via integrating an infinite chain of interactions involving intra- and inter-molecular sites. In this study, we have used the well-established Kovalenko-Hirata (KH) closure relation for RISM calculations [17]:

$$g_\gamma(\mathbf{r}) = \begin{cases} \exp\big(-u_\gamma(\mathbf{r})/(\mathrm{k_B}T) + h_\gamma(\mathbf{r}) - c_\gamma(\mathbf{r})\big) & \text{for} \quad g_\gamma(\mathbf{r}) \le 1 \\ 1 - u_\gamma(\mathbf{r})/(\mathrm{k_B}T) + h_\gamma(\mathbf{r}) - c_\gamma(\mathbf{r}) & \text{for} \quad g_\gamma(\mathbf{r}) > 1 \end{cases}$$

where $u_\gamma(\boldsymbol{r})$ is the 3D solute-solvent interaction potential, $\mathrm{k_B}$ is the Boltzmann constant, and T is the temperature.

2.1. Molecular dynamics (MD) simulations: All the molecular dynamics simulations were performed using the GROMACS molecular dynamics engine [18]. The liquid states of eight carboxylic acids were simulated using the all-atom GAFF force field parameters [19,20]. The initial solvent boxes of 512 carboxylic acid molecules were equilibrated at 298K and 1 bar pressure with NVT and NPT equilibrium using a Berendsen thermostat without any restraints for each carboxylic acid. 10ns production simulations were performed on the equilibrated systems. The molecular (and atomic) distribution functions were computed from the production simulations using the standard utility codes provided in the GROMACS suite. The acetic acid-water mixture simulations were performed at various mole fraction compositions, viz. 0.1, 0.3. 0.5, 0.7, and 0.9 mole fractions of acetic acid in water. The water mixtures of TFA and TCA were calculated for 0.9, 0.7, and 0.5 mole fraction ratios of the corresponding acids.

2.2. RISM-KH calculations: The lowest energy conformation of all the solutes, generated using the OpenBabel toolkit with MMFF94 force field, was further used for all the 3D-RISM-KH calculations [21]. The 3D-RISM-KH based excess chemical potential and partial molar volume (used as descriptors in the prediction) were calculated using the

rism1d code implemented in the AMBERTOOLS suite of programs [22]. We used a united atom AMBER force field parameter for all the liquid carboxylic acids (C2-C6 and trihalo acetic acids) in combination with the AM1-BCC charges [23,24]. The force field parameters used for the RISM calculations are provided in Table 1. The partial atomic charges of all non-acidic hydrogens, except for formic acid, are summed to that of the carbon atom to which the H-atom(s) are directly bonded. The extended-RISM (X-RISM) formalism was used to calculate the susceptibility functions of carboxylic acid molecules [25]. For the susceptibility calculations of the liquid aqueous mixtures of acetic acid, the dielectric-RISM (D-RISM) formalism was used with the modified TIP3P forcefield parameters [26].

Table 1. Force field parameters used in the RISM simulations.

Atom Type	Mass (amu)	σ (Å)	ε (kcal/mol)
O[—H, carboxylic]	16.000	1.7210	0.2104
O[=C]	16.000	1.6612	0.2100
C[H_2]	14.026	2.0580	0.1094
C[H_3]	15.034	2.0580	0.1494
$C_{carboxylic}$	12.010	1.9080	0.0860
H_{formic}	1.008	1.359	0.0150
H_{acid}	1.008	0.6288	0.02104
O_{water}	16.000	1.7683	0.1520
H_{water}	1.008	0.6939	0.0152
F	19.000	1.7500	0.06999
Cl	35.450	1.9480	2.6500

2.3. Density functional theory (DFT) calculations: The liquid structures of acetic acid, trifluoro-, and trichloro-acetic acids were further explored using the density functional theory. The B3LYP density functional with the correlation consistent cc-pVTZ basis set was used for all the calculations [27-30]. All the structures were confirmed as minima on respective potential energy surfaces through vibrational modes analysis. The dimeric and multimeric form of the

AcOH and water mixtures were calculated using the SMD solvation model in acetic acid continuum [31]. For the TFA and TCA systems, all the calculations are done in gas phase, as no continuum models of these acids are available for electronic structure calculations. All the interaction energies reported involve the zero point energy. The Gaussian16 suit of quantum chemical programs was used for all the DFT calculations [32].

3. Results and Discussion

The results and discussions are divided into four sections. The first section details the liquid structures of C1-C6 carboxylic acids obtained from the MD and RISM simulations. The second section is devoted to the structure of the liquid trifluoro- and trichloroacetic acids. The third section details the structure of the aqueous mixtures of acetic acid and trifluoro acetic acid. The final section focuses on the neat liquid forms and water mixtures of acetic acid, trifluoro and trichloro acetic acid obtained using the DFT calculations. The MD simulations of the carboxylic acids were evaluated by comparing the densities of the equilibrated pure liquids from the simulations with those reported in the literature (Table 2). The density profiles are provided in the supplementary materials. These equilibrated systems were further analyzed for distribution function calculations.

Table 2. MD simulated and reference densities (ρ in gm/cm^3) of carboxylic acids used in this study at 298K.

Molecule	ρ (MD Simulation)[a]	ρ (Reference)[b]
Formic acid (C1)	1.28 (±0.010)	1.22 (33)
Acetic acid (C2, AcOH)	1.08 (±0.012)	1.05 (33)
Propanoic acid (C3)	1.01 (±0.007)	0.99 (34)
Butanoic acid (C4)	0.97 (±0.006)	0.96 (35)
Pentanoic acid (C5)	0.94 (±0.008)	0.94 (35)
Hexanoic acid (C6)	0.92 (±0.018)	0.93 (36)
Trifluoroacetic acid (TFA)	1.52 (±0.006)	1.53 (35)
Trichloroacetic acid (TCA)	1.68 (±0.003)	1.61 (37)

[a]Error in calculation. [b]Reference cited.

The qualitative nature of the radial distribution function plots obtained from the MD simulations using the all-atom GAFF force field are similar to the partial distribution plots from the RISM calculations with the united atom AMBER force field, with reference to the positions of the peaks. There are several differences noted between the MD generated RDFs and the RISM generated PDFs in terms of the fine structures. All the six carboxylic acids showed presence of chain-like structures in the liquid form characterized by the -O-H1···O= interaction (H1-O1 rdf plots, Figure 2). The first maxima in g_{H1O1} plots are at ~2.6Å, followed by another peak around ~3Å and a broad hump at ~4-6Å. Other broad regions were observed spanning to ~9Å for carboxylic acids C3 to C6. The multiple peaks may signify the presence of different clusters, e.g. chain and rings, in the liquid states held together by hydrogen bond(s) between neighboring molecules. The intensity of the peak ~3Å gradually decreases with the increasing length of the aliphatic tail. The significant contribution of the O(=C)···H interaction in the region of 2.6-2.8Å is also reported from the diffraction studies of formic acid [38]. Further, the shoulder around 3Å in the g_{OH} rdf was assigned to a cyclic dimer structure [8]. Such cyclic structures were noted for AcOH also [39]. Interestingly, Raman spectroscopic studies have pointed to cooperative existence of cyclic and linear dimers of AcOH with dissociated monomers in the liquid state [40]. The local order in liquid AcOH was attributed to cyclic and linear trimers in the previous studies [41,42]. The 1D-RISM calculation also picked up such intermolecular structures with a maximum at ~2.5Å and a broad hump spanning in 3-6Å region for all the six aliphatic carboxylic acids. The intermolecular interaction between H1···O atoms (H1-O rdf plots) is complicated in nature. There is a small minimum around ~2.2Å in the g_{H1O} rdf plots followed by multiple maxima around ~3-4.5Å for all the six acids (Figure 2). The RISM partial distribution functions picked up these interactions in the aforementioned region. The broad shape of the RISM peaks is expected and observed in the previous calculations, too. The partial distribution functions of the carboxyl carbon showed comparable profiles between the MD and RISM simulations (see the supplementary materials). Overall, the simulation profiles from the MD and RISM simulations featured multimeric structures of the six carboxylic acids under study. These multimeric forms can be chain like as well as ring like structures (vide infra).

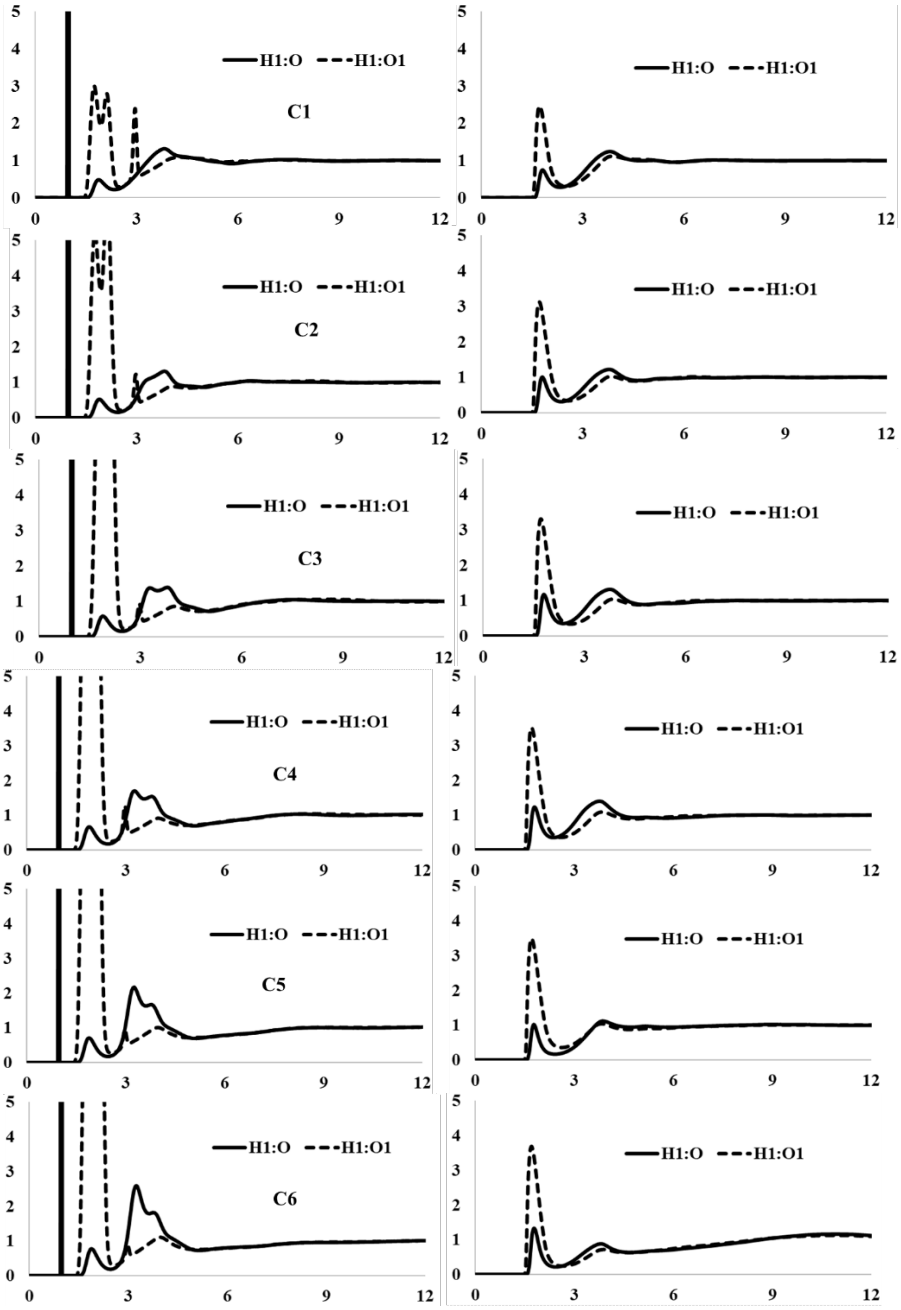

Figure 2. Radial distribution function (rdf) plots from the MD simulations (left panel) and the partial distribution function (PDF) plots from the RISM calculations (right panels) for the six aliphatic carboxylic acids.

The MD and RISM computed distribution function plots for H1···O and H1···O1 intermolecular interactions for TFA and TCA are similar to those of the other six acids. The H1···F interaction showed multiple minima in the 3-6Å region, in the MD simulation. The RISM computation of this distribution function yielded the first minimum at ~2.5Å

followed by a broad one in 3-6Å region (Figure 3). The presence of multimeric structures involving intermolecular H···F interaction are predicted in these calculations. The H1···Cl interaction profiles showed multiple minima at 3-6Å region in the MD profile and a broad peak in the RISM calculations. The result presented here agree with the previous report on TFA [38].

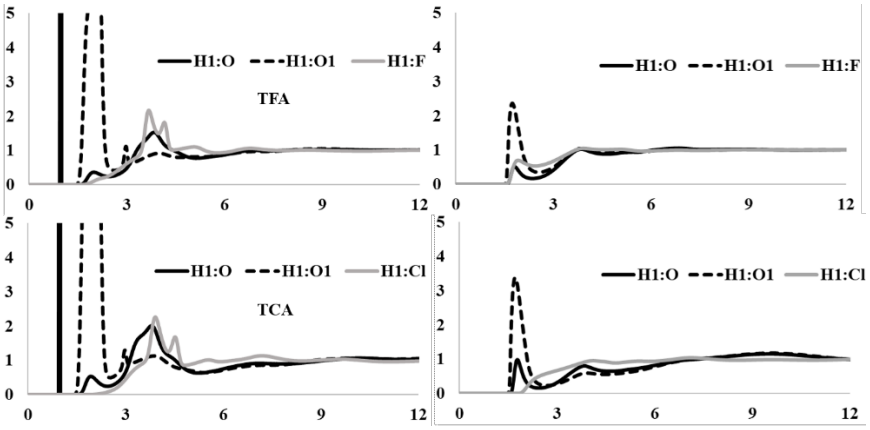

Figure 3. Radial distribution function (rdf) plots from the MD simulations (left panel) and the partial distribution function (PDF) plots from the RISM calculations (right panels) of trifluoro acetic acid (TFA) and trichloroacetic acid (TCA).

The AcOH-water mixtures have evolving H1(carboxylic)···O(water) hydrogen bonds with the increasing concentration of the water in the mixtures studied using the MD simulations, as evident from Figures 4 and 5. The H1···O(=C) rdf has the highest intensity with maximum water concentration, probably due to disruption of the AcOH clusters by the H1···O(water) interactions and making the carbonyl oxygen relatively more available for intermolecular interactions. The water hydrogens interactions with both the oxygens of AcOH increase with the increasing water concentrations with the first maxima arising around ~2 Å. The findings are in line with the previous reports on the mixture of AcOH with water. These findings are in line with the experimental findings [43]. The intermolecular H-bonding between the carboxylic ends in the dimeric structures of AcOH in hydrated conditions were reported to be linear by Imbreti and co-workers [43]. The stabilization of strong dipole dimeric acetic acid structures by hydration was supported by the RISM-SCF calculations, too [44]. The RISM computations of the mixture qualitatively agrees with the MD simulation profiles (Figure 5). A close inspection of Figure 5 also reveals some interesting differences between the MD rdfs and the RISM computed partial distribution functions. The maxima in the PDFs for the 1:1

mixture of AcOH-water is moved toward the distance shorter than for other concentrations. The effect of increasing water concentration was not well resolved from the PDFs obtained using the RISM formalism. The maxima of the PDFs for H1···O(water) follow the pattern similar as observed from the MD simulations.

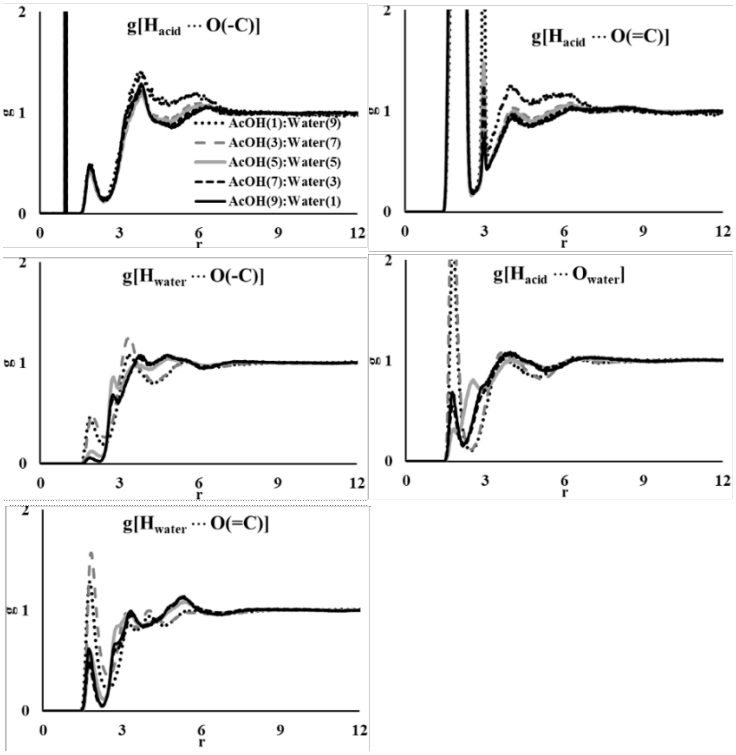

Figure 4. Radial distribution function (rdf) plots from the MD simulations of the AcOH-water mixture.

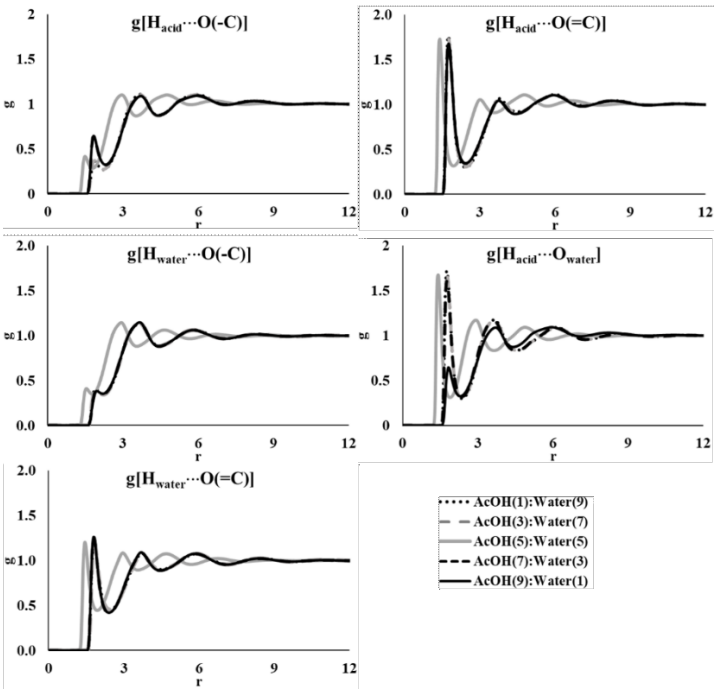

Figure 5. Partial distribution function (PDF) plots from the RISM calculations of the AcOH-water mixture.

The simulations of the TFA-water and TCA-water mixtures were conducted for three concentrations of acids, viz. 0.9, 0.7, and 0.5 mole in the corresponding mixture. The intermolecular hydrogen bonding between carboxylic acid and water molecule increases with increasing water concentrations, as evident from the rdf plots. The F···H(water) interaction did not show much dependence on the water concentration, with a double peak maximum between 3.5-4.4Å (Figure 6). The weakening of the dimer structure of TFA in the presence of water molecules were previously reported from the large-angle X-ray scattering and NMR experiments [45]. For the TCA, the acid-water hydrogen bonds are shifted towards longer separation for higher water concentrations (Figure 7), although the overall peak positions between TFA-water and TCA-water mixtures appear in a similar separation. The Cl···H(water) interactions are not as well defined as for the fluorinated acid with broad shoulders spanning between 3-6 Å. The RISM computed maxima on the PDFs are in good agreement with the MD computed data, although the effect of increasing water concentrations was not resolved in the RISM computed PDFs.

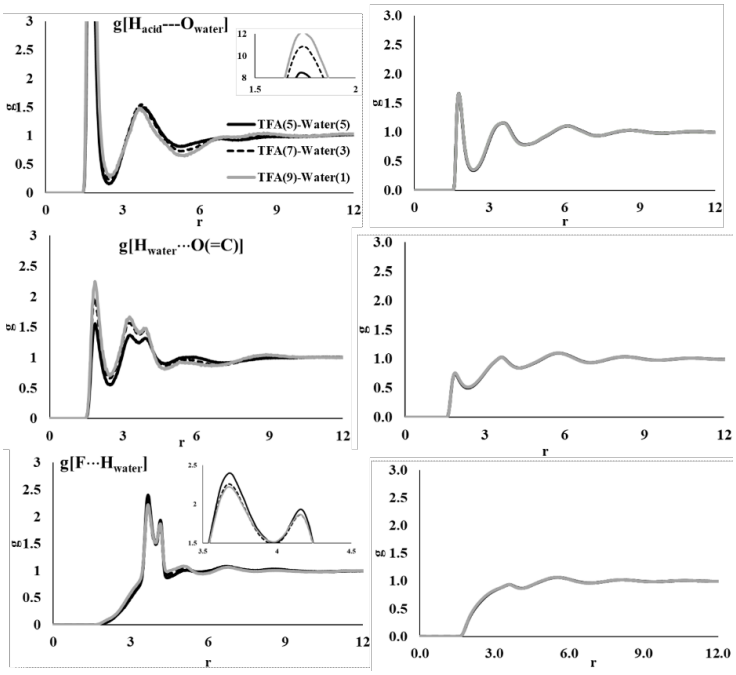

Figure 6. Radial distribution function (rdf) plots from the MD simulations (left panel) and the partial distribution function (PDF) plots from the RISM calculations (right panels) of trifluoro acetic acid (TFA).

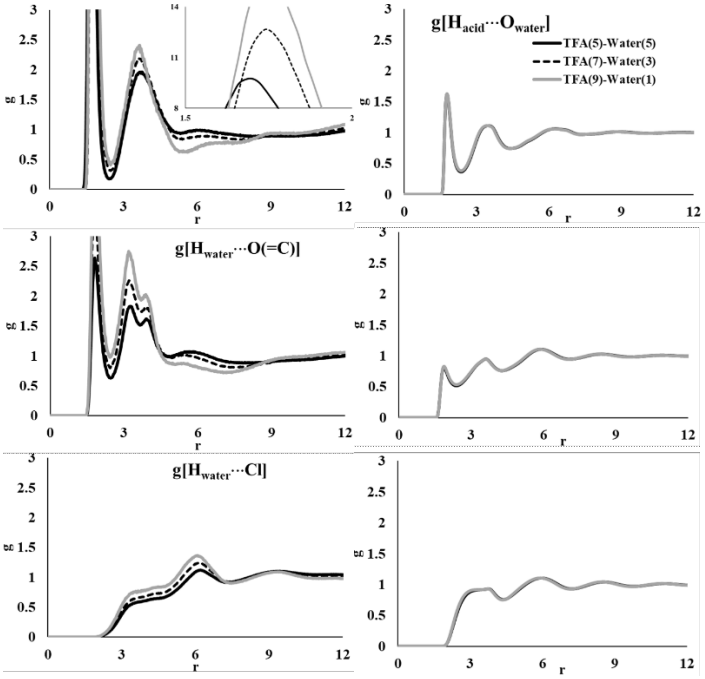

Figure 7. Radial distribution function (rdf) plots from the MD simulations (left panel) and the partial distribution function (PDF) plots from the RISM calculations (right panels) of trichloro acetic acid (TCA).

We have used the hybrid B3LYP density functional to explore possible multimeric forms of the AcOH, TFA, and TCA as well as the water bound structures. The intermolecular H(carboxylic)···O(=C) distances were found in the range of 1.64-1.77Å, depending on the number of AcOH units involved (Figure 8). The most stable dimeric structure of AcOH in the liquid state is the cyclic structure (A2_2). We were able to obtain two different forms of the trimeric structures. One of the trimers (A3_1) was an open chain structure held together by H-bonds involving carboxylic acid groups and a possible interaction between O(=C) and methyl hydrogens. The other trimeric form (A3_2) has a cyclic structure of H-bonds among carboxylic ends. These two structures differ by ~2 kcal/mol in the stabilization energy favoring the later. The non-symmetrical tetrameric form (A4) of the AcOH was also found to be cyclic using the DFT calculations. The water molecule can effectively work as a bridging unit between neighboring AcOH molecules by providing an extended H-bond network. The DFT optimized structures of the hydrated AcOH monomers and dimers have water making hydrogen bonds with neighboring AcOH molecules. This calculation supports the hypothesis that water molecules disrupt the H-bonding network between the AcOH molecules by inserting themselves into the ring and/or chain structures of carboxylic acid multimers. There are reports on the structure of the hydrated acetic acid monomers and dimers from quantum chemical calculations in the gas phase using DFTB-D and post-Hartree-Fock methods [46-48]. These reports suggest the cyclic dimer as the predominant form. The stability of microhydrated AcOH molecules were also reported from DFTB-D dynamics calculations [49]. The experimental association free energy of the AcOH dimers were reported to be in the range of 0-2 kcal/mol [50-52]. We have obtained a range of 0-4.4 kcal/mol of free energy of association from our DFT calculations in the liquid continuum model for the AcOH dimers (Table 3).

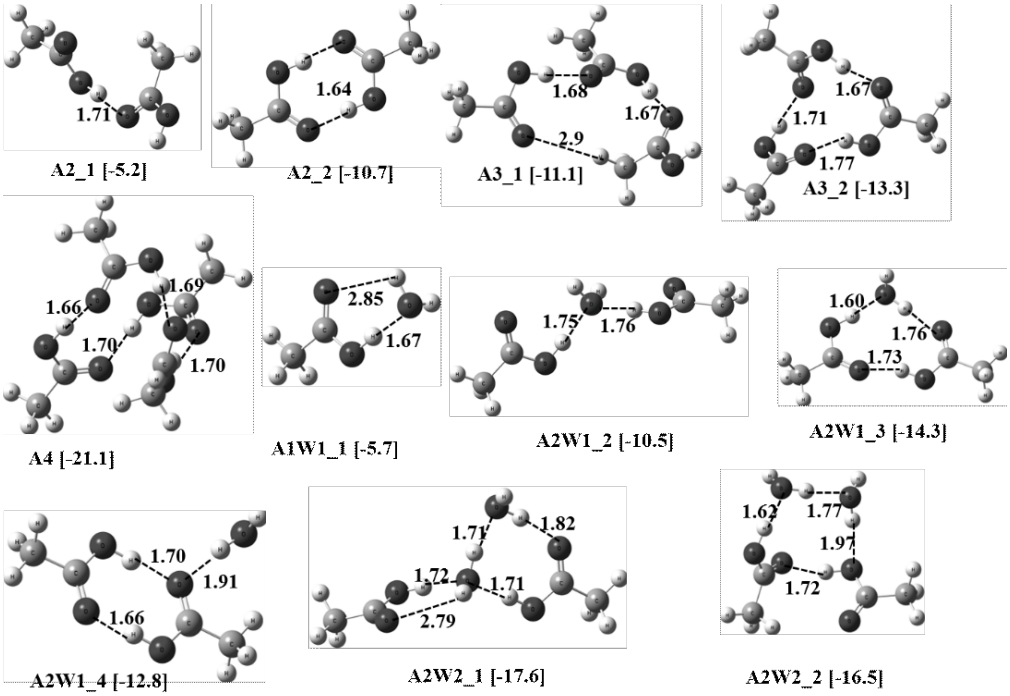

Figure 8. SMD//B3LYP/cc-pVTZ optimized geometries of the lowest energy multimers of the liquid acetic acid (A) and water(W) bound structures. The interaction energies, in kcal/mol, are provided in parentheses. Atom color code: white, Hydrogen; gray, Carbon; black, Oxygen.

The most stable dimers of the TFA and TCA molecules are cyclic ones, like the AcOH units, as obtained from the DFT calculations. The H-bonding distances between the three acids, viz. AcOH, TFA, and TCA, are comparable. The tetrameric form of the TFA was symmetric, while the same for TCA has a non-planar ring structure involving the carboxyl terminal H-bond network. In these gas phase calculations, all the lowest energy structures of the hydrated TFA and TCA monomeric and multimeric units have hydrogen bonding involving the carboxyl end of the acid and water molecules but not involving the halide atom and water hydrogen atoms. The DFT optimized geometries are summarized in Figures 9 and 10. The free energy of association for the tetrameric TFA is found to be favorable via the DFT calculations.

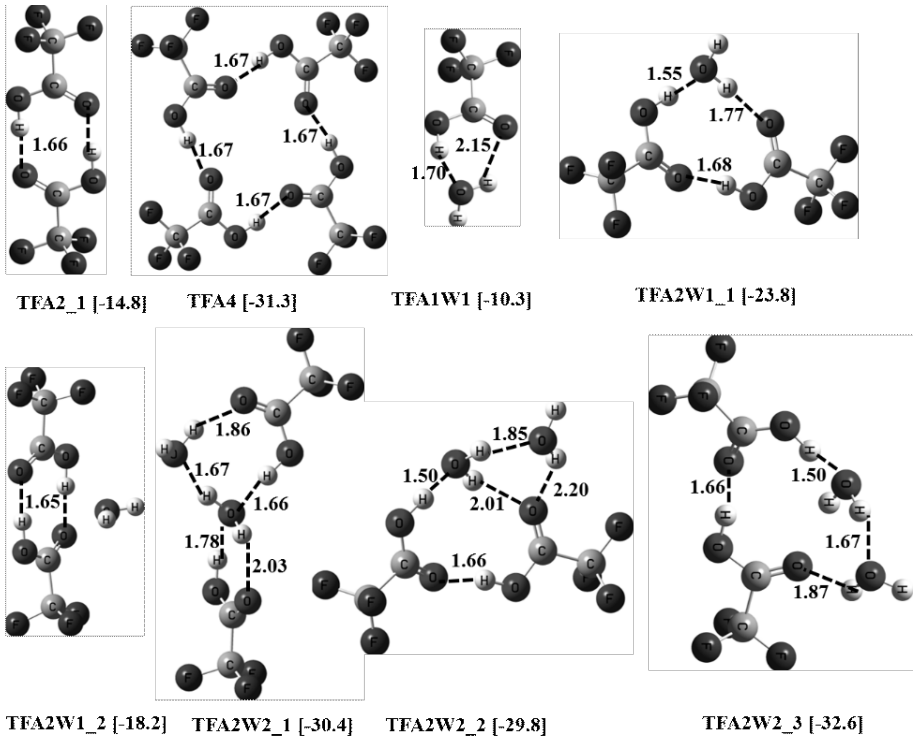

Figure 9. B3LYP/cc-pVTZ optimized geometries of the lowest energy multimers of the liquid trifluoro acetic acid (TFA) and water (W) bound structures. The interaction energies, in kcal/mol, are provided in parentheses. Atoms are labeled for clarity.

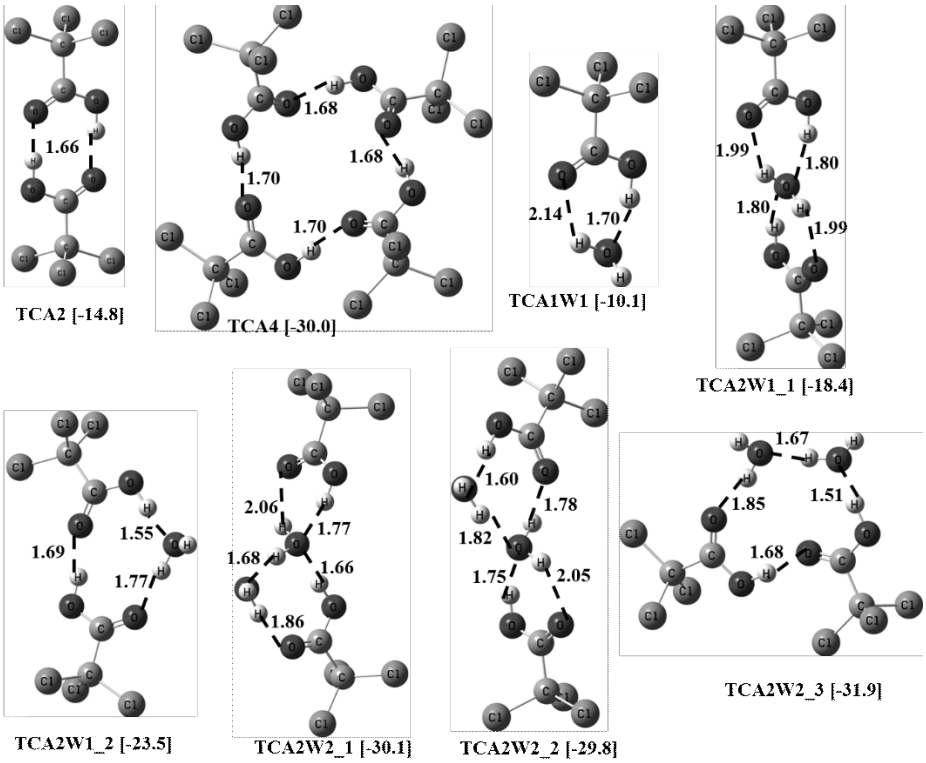

Figure 10. B3LYP/cc-pVTZ optimized geometries of the lowest energy multimers of the liquid trifluoro acetic acid (TFA) and water(W) bound structures. The interaction energies, in kcal/mol, are provided in parentheses. Atoms are labeled for clarity.

Table 3. Interaction energetics (in kcal/mol) computed using the B3LYP/cc-pVTZ method.

System	ΔH	ΔG	System	ΔH	ΔG
A2_1[a]	-4.8	4.4	TFA2W1_1	-24.1	-5.0
A2_2[a]	-10.6	-0.3	TFA2W1_2	-17.7	-0.5
A3_1[a]	-10.3	8.4	TFA2W2_1	-31.0	-3.6
A3_2[a]	-12.3	6.7	TFA2W2_2	-30.9	-2.6
A4[a]	-20.2	11.0	TFA2W2_3	-33.4	-5.4
A1W1_1[a]	-6.1	2.4	TCA2_1	-14.6	-4.0

A2W1_2[a]	-10.5	6.3	TCA4	-28.9	2.4
A2W1_3[a]	-14.6	3.3	TCA1W1	-10.7	-1.6
A2W1_4[a]	-12.9	5.5	TCA2W1_1	-18.8	0.1
A2W2_1[a]	-18.5	8.3	TCA2W1_2	-23.7	-4.8
A2W2_2[a]	-17.1	9.6	TCA2W2_1	-26.5	-3.1
TFA2_1	-14.6	-3.7	TCA2W2_2	-26.1	-2.6
TFA4	-29.8	-1.5	TCA2W2_3	-27.8	-5.0
TFA1W1	-10.8	-1.7			

[a]Computed at the SMD/B3LYP/cc-pvTZ level with the acetic acid continuum model.

4. Conclusion

In this report, we have used different computational chemistry methods, e.g. molecular dynamics simulations, RISM calculations, and DFT methods to explore the liquid states of straight chain aliphatic carboxylic acids (C1-C6) and trifluoro- and trichloro acetic acid. Further, water mixtures of the acetic acid and tri-halo acetic acids were also examined. We have used the united atom AMBER force field for the RISM calculations. The all-atom MD simulations were done using the GAFF force field with the AM1-BCC atomic charges. The molecular simulations and RISM calculations are qualitatively comparable. The aliphatic carboxylic acids make chain and ring like structures in the liquid states. Upon introduction of the water into pure liquid acid medium, these multimeric acid forms are destroyed as water molecule(s) is inserted between neighboring carboxylic acids. The water molecules make H-bond bridges between -COOH groups. The presence of chain-like and ring-like multimeric structures in pure liquid acids as well as hydrated forms is further verified using the DFT calculations. The RISM methods failed to resolve the effect of increasing water concentration on the carboxylic-acid structure.

Conflict of Interest: The authors have no conflict of interest to declare.

Supplementary materials:

Temperature and density profile from the equilibration simulations, DFT optimized coordinates

Acknowledgements:

This work was financially supported by the NSERC Discovery Grant (RES0029477), and Canadian Consortium on Neurodegeneration in Aging (CCNA) Protein Misfolding, Phase II Grant (RES0051206). Generous computing time provided by WestGrid (www.westgrid.ca) and Compute Canada/Calcul Canada (www.computecanada.ca) is acknowledged.

References:

1. S. Ferrero, L. Zamirri, C. Ceccarelli, A. Witzel, A. Rimol, P. Ugliengo, Binding Energies of Interstellar Molecules on Crystalline and Amorphous Models of Water Ice by Ab Initio Calculations, Astrophys. J. 904 (2020) 11. https://doi.org/10.3847/1538-4357/abb953.

2. S.A. Sandford, M. Nuevo, P.P. Bera, and T.J. Lee, Prebiotic Astrochemistry and the Formation of Molecules of Astrobiological Interest in Interstellar Clouds and Protostellar Disks, Chem. Rev. 120 (2020) 4616-4659. DOI: 10.1021/acs.chemrev.9b00560.

3. G. Kamath, F. Cao, J.J. Potoff, An Improved Force Field for the Prediction of the Vapor−Liquid Equilibria for Carboxylic Acids, J. Phys. Chem. B 108 (2004) 14130–14136. https://doi.org/10.1021/jp048581s.

4. V.T. Lim, C.I. Bayly, L. Fusti-Molnar, D.L. Mobley, Assessing the Conformational Equilibrium of Carboxylic Acid via QM and MD Studies on Acetic Acid, J. Chem. Inf. Model. 59 (2019) 1957–1964. https://dx.doi.org/10.1021%2Facs.jcim.8b00835.

5. S, Riniker, B.A.C. Horta, B. Thijssen, S. Gupta, W.F. van Gunsteren, P.H. Hünenberger, Temperature dependence of the dielectric permittivity of acetic acid, propionic acid and their methyl esters: a molecular dynamics simulation study, Chemphyschem 13 (2012) 1182-90. doi: 10.1002/cphc.201100949.

6. S. Clifford, K. Bolton, D. Ramjugernath, Monte Carlo Simulation of Carboxylic Acid Phase Equilibria, J. Phys. Chem. B 110 (2006) 21938–21943. https://doi.org/10.1021/jp0625053.

7. T. Nakabayashi, K. Kosugi, N. Nishi, Liquid Structure of Acetic Acid Studied by Raman Spectroscopy and Ab Initio Molecular Orbital Calculations, J. Phys. Chem. A 103 (1999) 8595-8603. https://doi.org/10.1021/jp991501d.

8. R. Chelli, R. Righini, S. Califano, Structure of Liquid Formic Acid Investigated by First Principle and Classical Molecular Dynamics Simulations, J. Phys. Chem. B 109 (2005) 17006-17013. DOI: 10.1021/jp051731u.

9. A. Aerts, P. Carbonnière, F. Richter, A. Brown, Vibrational states of deuterated trans- and cis-formic acid: DCOOH, HCOOD, and DCOOD, 152 (2020) 024305, https://doi.org/10.1063/1.5135571.

10. D. Chandler, H.C. Anderson, Optimized cluster expansions for classical fluids. II. Theory of molecular liquids, J. Chem. Phys. 57 (1972) 1930. https://doi.org/10.1063/1.1678513.

11. D. Chandler, Derivation of an integral equation for pair correlation functions in molecular fluids, J. Chem. Phys. 59 (1973) 2742. https://doi.org/10.1063/1.1680393.

12. D. Chandler, J.D. McCoy, S.J. Singer, Density functional theory of nonuniform polyatomic systems. I. General formulation, J. Chem. Phys. 85 (1985) 5971. https://doi.org/10.1063/1.451510.

13. D. Chandler, J.D. McCoy, S.J. Singer, Density functional theory of nonuniform polyatomic systems. II. Rational closures for integral equations, J. Chem. Phys. 85 (1986) 5977. https://doi.org/10.1063/1.451511.

14. D. Chandler, Equilibrium structure and molecular motion in liquids, Acc. Chem. Res. 7 (1974) 246–251. https://doi.org/10.1021/ar50080a002.

15. A. Kovalenko, Molecular theory of solvation: Methodology summary and illustrations, Cond. Matt. Phys. 18 (2015) 32601. https://doi.org/10.5488/CMP.18.32601.

16. D. Roy, A. Kovalenko, 3D-RISM-KH Molecular Solvation Theory, in: D.R. Salahub, D. Wei (Eds.),

Multiscale Dynamics Simulations: Nano and Nano-bio Systems in Complex Environments, RSC Publishing, London, 2021, pp. 254–286. https://doi.org/10.1039/9781839164668-00254.

17. A. Kovalenko, F. Hirata, Potential of mean force between two molecular ions in a polar molecular solvent: A study by the three-dimensional reference interaction site model, J. Phys. Chem. B 103 (1999) 7942–7957. https://doi.org/10.1021/jp991300+

18. M.J. Abraham, T. Murtola, R. Schulz, S. Páll, J.C. Smith, B. Hess, E. Lindahl, GROMACS: High performance molecular simulations through multi-level parallelism from laptops to supercomputers, SoftwareX 1-2 (2015) 19-25. https://doi.org/10.1016/j.softx.2015.06.001.

19. J. Wang, W. Wang, P.A. Kollman, D.A. Case, Automatic atom type and bond type perception in molecular mechanical calculations, J. Mol. Graph. Model. 25 (2006) 247260. doi: 10.1016/j.jmgm.2005.12.005.

20. J. Wang, R.M. Wolf, J.W. Caldwell, P.A. Kollman, D.A. Case, Development and testing of a general amber force field, J. Comput. Chem. 25 (2004) 1157-1174. doi: 10.1002/jcc.20035.

21. N.M. O'Boyle, M. Banck, C.A. James, C. Morley, T. Vandermeersch, G.R. Hutchison, Open Babel: An open chemical toolbox, J. Cheminform. 3 (2011) 33. https://doi.org/10.1186/1758-2946-3-33.

22. D.A. Case, H.M. Aktulga, K. Belfon, I.Y. Ben-Shalom, S.R. Brozell, D.S. Cerutti, T.E. Cheatham, III, V.W.D. Cruzeiro, T.A. Darden, R.E. Duke, G. Giambasu, M.K. Gilson, H. Gohlke, A.W. Goetz, R. Harris, S. Izadi, S.A. Izmailov, C. Jin, K. Kasavajhala, M.C. Kaymak, E. King, A. Kovalenko, T. Kurtzman, T.S. Lee, S. LeGrand, P. Li, C. Lin, J. Liu, T. Luchko, R. Luo, M. Machado, V. Man, M. Manathunga, K.M. Merz, Y. Miao, O. Mikhailovskii, G. Monard, H. Nguyen, K.A. O'Hearn, A. Onufriev, F. Pan, S. Pantano, R. Qi, A. Rahnamoun, D.R. Roe, A. Roitberg, C. Sagui, S. Schott-Verdugo, J. Shen, C.L. Simmerling, N.R. Skrynnikov, J. Smith, J. Swails, R.C. Walker, J. Wang, H. Wei, R.M. Wolf, X. Wu, Y. Xue, D.M. York, S. Zhao, P.A. Kollman, Amber 2021, University of California, San Francisco.

23. L. Yang, C. Tan, M.-J. Hsieh, J. Wang, Y. Duan, P. Cieplak, J. Caldwell, P.A. Kollman, R. Luo, New-Generation Amber United-Atom Force Field, J. Phys. Chem. B 110 (2006) 13166–13176. https://doi.org/10.1021/jp060163v.

24. A. Jakalian, D.B. Jack, C.I. Bayly, Fast, efficient generation of high-quality atomic charges. AM1-BCC model: II. Parameterization and validation, J. Comput. Chem. 23 (2002) 1623-41. doi: 10.1002/jcc.10128.

25. F. Hirata, P.J. Rossky, An extended rism equation for molecular polar fluids, Chem. Phys. Lett. 83 (1981) 329-334. https://doi.org/10.1016/0009-2614(81)85474-7.

26. T. Luchko, S. Gusarov, D.R. Roe, C. Simmerling, D.A. Case, J. Tuszynski, A. Kovalenko, Three-dimensional molecular theory of solvation coupled with molecular dynamics in Amber, J. Chem. Theory Comput. 6 (2010) 607–624. https://doi.org/10.1021/ct900460m.

27. A.D. Becke, Density-functional exchange-energy approximation with correct asymptotic-behavior, Phys. Rev. A 38 (1988) 3098-100.

28. C. Lee, W. Yang, R.G. Parr, Development of the Colle-Salvetti correlation-energy formula into a functional of the electron density, Phys. Rev. B, 37 (1988) 785-89.

29. T.H. Dunning Jr., Gaussian basis sets for use in correlated molecular calculations. I. The atoms boron through neon and hydrogen, J. Chem. Phys. 90 (1989) 1007-23.

30. D.E. Woon, T.H. Dunning Jr., Gaussian-basis sets for use in correlated molecular calculations. 3. The atoms aluminum through argon, J. Chem. Phys. 98 (1993) 1358-71.

31. A.V. Marenich, C.J. Cramer, D.G. Truhlar, Universal solvation model based on solute electron density and a continuum model of the solvent defined by the bulk dielectric constant and atomic surface tensions, J. Phys. Chem. B 113 (2009) 6378-96.

32. Gaussian 16, Revision C.01, M. J. Frisch, G. W. Trucks, H. B. Schlegel, G. E. Scuseria, M. A. Robb, J. R. Cheeseman, G. Scalmani, V. Barone, G. A. Petersson, H. Nakatsuji, X. Li, M. Caricato, A. V. Marenich, J. Bloino, B. G. Janesko, R. Gomperts, B. Mennucci, H. P. Hratchian, J. V. Ortiz, A. F. Izmaylov, J. L. Sonnenberg, D. Williams-Young, F. Ding, F. Lipparini, F. Egidi, J. Goings, B. Peng, A. Petrone, T. Henderson, D. Ranasinghe, V. G. Zakrzewski, J. Gao, N. Rega, G. Zheng, W. Liang, M. Hada, M. Ehara, K. Toyota, R. Fukuda, J. Hasegawa, M. Ishida, T. Nakajima, Y. Honda, O. Kitao, H. Nakai, T. Vreven, K. Throssell, J. A. Montgomery, Jr., J. E. Peralta, F. Ogliaro, M. J. Bearpark, J. J. Heyd, E. N. Brothers, K. N. Kudin, V. N. Staroverov, T. A. Keith, R. Kobayashi, J. Normand, K. Raghavachari, A. P. Rendell, J. C. Burant, S. S. Iyengar, J. Tomasi, M. Cossi, J. M. Millam, M. Klene, C. Adamo, R. Cammi, J. W. Ochterski, R. L. Martin, K. Morokuma, O. Farkas, J. B. Foresman, D. J. Fox, Gaussian 16, rev. B.01, Gaussian, Inc., Wallingford CT, 2016.

33. W.M. Haynes, (ed.) CRC Handbook of Chemistry and Physics. 91st ed. CRC Press Inc., Florida, 2010-2011.

34. W. Gerhartz, (exec ed.), Ullmann's Encyclopedia of Industrial Chemistry. 5th ed. Vol A1: VCH Publishers, Florida, 1993.

35. M.J. O'Neil,(ed.), The Merck Index - An Encyclopedia of Chemicals, Drugs, and Biologicals. 13th Edition, Whitehouse Station, NJ: Merck and Co., Inc., 2001.

36. Kirk-Othmer Encyclopedia of Chemical Technology, 4th ed. Volumes 1, John Wiley and Sons, New York, 1993.

37. D.R. Lide, CRC Handbook of Chemistry and Physics, 86TH Edition, CRC Press, Taylor & Francis, Boca Raton, Florida, 2005.

38. J. Karle and L. O. Brockway, An Electron Diffraction Investigation of the Monomers and Dimers of Formic, Acetic and Trifluoroacetic Acids and the Dimer of Deuterium Acetate, J. Am. Chem. Soc. 66 (1944) 574–584. https://doi.org/10.1021/ja01232a022.

39. S. Imberti, D.T. Bowron, Formic and acetic acid aggregation in the liquid state, J. Phys.: Condens. Matter 22 (2010) 404212. https://doi.org/10.1088/0953-8984/22/40/404212.

40. J. Wu, Gaussian analysis of Raman spectroscopy of acetic acid reveals a significant amount of monomers that effectively cooperate with hydrogen bonded linear chains, Phys.Chem.Chem.Phys. 16 (2014) 22458. DOI: 10.1039/c4cp03999h.

41. S. Fathi, S. Bouazizi, S. Trabelsi, M.A. Gonzalez, M. Bahri, S. Nasr, M.-C. Bellissent-Funel, Structural investigation of liquid acetic acid by neutron scattering, DFT calculations and molecular dynamics simulations. Complementarity to x-ray scattering results, J. Mol. Liquid. 196 (2014) 69–76. https://doi.org/10.1016/j.molliq.2014.02.043

42. A. Chebaane, S. Trabelsi, S. Nasr, M.-C. Bellissent-Funel, Local order in fully deuterated liquid acetic acid as studied by neutron scattering. Complementarity to X-ray results, J. Mol. Liquid. 198 (2014) 204–210. https://doi.org/10.1016/j.molliq.2014.06.029

43. S. Soffientini, L. Bernasconi, S. Imberti, The hydration of formic acid and acetic acid, J. Mol. Liquid. 205 (2015) 85-92. https://doi.org/10.1016/j.molliq.2014.11.030.

44. T. Nakabayashi, H. Sato, F. Hirata, N. Nishi, Theoretical Study on the Structures and Energies of Acetic Acid Dimers in Aqueous Solution, J. Phys. Chem. A 105 (2001) 245–250. https://doi.org/10.1021/jp0030239.

45. T. Takamuku, Y. Kyoshoin, H. Noguchi, S. Kusano, T. Yamaguchi, Liquid Structure of Acetic Acid−Water and Trifluoroacetic Acid−Water Mixtures Studied by Large-Angle X-ray Scattering and NMR, J. Phys. Chem. B 111 (2007) 9270–9280. https://doi.org/10.1021/jp0724976.

46. M. Zhang, L. Chen, H. Yang, J. Ma, Theoretical Study of Acetic Acid Association Based on Hydrogen Bonding Mechanism, J. Phys. Chem. A. 121 (2017) 4560−4568. https://doi.org/10.1021/acs.jpca.7b03324.

47. L. Pu, Y. Sun, and Z. Zhang, Hydrogen Bonding of Hydrates of Double Acetic Acid Molecules, J. Phys. Chem. A 113 (2009) 6841–6848. DOI: 10.1021/jp902634h.

48. L. Pu, Y. Sun, Z. Zhang, Hydrogen Bonding in Hydrates with one Acetic Acid Molecule, J. Phys. Chem. A 2010, 114, 10842–10849. DOI:10.1021/jp103331a.

49. H. Pašalić, D. Tunega, A.J.A. Aquino, G. Haberhauer, M.H. Gerzabek, H. Lischka, The stability of the acetic acid dimer in microhydrated environments and in aqueous solution, Phys. Chem. Chem. Phys. 14 (2012) 4162-4170. DOI: 10.1039/C2CP23015A

50. K. Yamamoto, N. Nishi, Hydrophobic hydration and hydrophobic interaction of carboxylic acids in aqueous solution: mass spectrometric analysis of liquid fragments isolated as clusters, J. Am. Chem. Soc. 112 (1990) 549–558. DOI: 10.1021/ja00158a011.

51. J.B. Ng, H.F. Shurvell, Application of factor analysis and band contour resolution techniques to the Raman spectra of acetic acid in aqueous solution. J. Phys. Chem. 91 (1987) 496–500. DOI: 10.1021/j100286a046.

52. E.E. Schrier, M. Pottle, and H.A. Scheraga, The Influence of Hydrogen and Hydrophobic Bonds on the Stability of the Carboxylic Acid Dimers in Aqueous Solution, J. Am. Chem. Soc. 86 (1964) 3444–3449. DOI: 10.1021/ja01071a009.